Optical Engineering

OpticalEngineering.SPIEDigitalLibrary.org

Fresnel spatial filtering of quasihomogeneous sources for wave optics simulations

Milo W. Hyde, IV
Santasri R. Bose-Pillai

SPIE.

Milo W. Hyde, , IVSantasri R. Bose-Pillai, "Fresnel spatial filtering of quasihomogeneous sources for wave optics simulations," *Opt. Eng.* **56**(8), 083107 (2017), doi: 10.1117/1.OE.56.8.083107.

Fresnel spatial filtering of quasihomogeneous sources for wave optics simulations

Milo W. Hyde IV[a,*] **and Santasri R. Bose-Pillai**[b,c]
[a]Air Force Institute of Technology, Department of Electrical and Computer Engineering, Dayton, Ohio, United States
[b]Air Force Institute of Technology, Department of Engineering Physics, Dayton, Ohio, United States
[c]Srisys Inc., West Chester Township, Ohio, United States

Abstract. High-spatial-frequency optical fields or sources are often encountered when simulating directed energy, active imaging, or remote sensing systems and scenarios. These spatially broadband fields are a challenge in wave optics simulations because the sampling required to represent and then propagate these fields without aliasing is often impractical. To address this, two spatial filtering techniques are presented. The first, called Fresnel spatial filtering, finds a spatially band-limited source that, after propagation, produces the exact observation plane field as the broadband source over a user-specified region of interest. The second, called statistical or quasihomogeneous spatial filtering, finds a spatially band-limited source that, after propagation and over a specified region of interest, yields an observation plane field that is statistically representative of that produced by the original broadband source. The pros and cons of both approaches are discussed in detail. A wave optics simulation of light transiting a ground glass diffuser and then propagating to an observation plane in the near-zone is performed to validate the two filtering approaches. © *The Authors. Published by SPIE under a Creative Commons Attribution 3.0 Unported License. Distribution or reproduction of this work in whole or in part requires full attribution of the original publication, including its DOI.* [DOI: 10.1117/1.OE.56.8.083107]

Keywords: coherence; Fresnel integral; optical simulations; rough surface scattering; statistical optics.

Paper 170746 received May 16, 2017; accepted for publication Jul. 26, 2017; published online Aug. 24, 2017.

1 Introduction

Wave optics simulations are a critical part of optical system design and are used in practically every discipline, including light propagation in random or nonlinear media, rough surface scattering, guided-wave propagation, etc.[1–3] The simulation of high-spatial-frequency or spatially broadband optical fields is generally a challenge because the sampling needed to represent and then propagate these fields (typically using fast Fourier transforms) on a discrete grid without aliasing can be prohibitive. The literature is replete with books and papers on this topic.[1–7]

The most intuitive and popular approach for dealing with spatially broadband fields or sources is to spatially filter the source (or the propagation kernel) prior to propagation.[1,3,7–10] While the details may differ, the goal of all spatial filtering approaches is the same: to find a spatially band-limited (or near-band-limited) source that produces the exact same observation field as the original, spatially broadband source over a specified region of interest (RoI).

Although spatial filtering is a common optical simulation technique, to the authors' knowledge, it has never been theoretically investigated starting from the Fresnel propagation integral. This analysis is presented in Sec. 2. The result, called Fresnel spatial filtering, is an integral expression that yields the spatially filtered source given the original field. This integral is discussed at length.

In only a few cases, the Fresnel filtering integral can be evaluated in closed form. Thus, a new statistical filtering method is also presented, which is broadly applicable in simulations involving random optical fields, e.g., scattering from rough surfaces, transmission through diffusers, transmission through turbid (highly scattering) media, etc. These situations are commonly encountered in optical phased array systems, high-energy laser weapons, active imaging, remote sensing, and medicine.

Both the field and statistical filtering approaches are validated in Sec. 3. For this purpose, the near-zone propagation of light transmitted by a ground glass diffuser is simulated. The results obtained using both approaches are compared to those of the original, spatially broadband field. Last, this paper is summarized, and a brief discussion of possible applications is provided.

2 Methodology

2.1 *Fresnel Spatial Filtering*

The field in the observation plane given the field in the source plane is

$$U^{\mathrm{obs}}(\boldsymbol{\rho}, z) = \frac{\exp(\mathrm{j}kz)\exp\left(\frac{\mathrm{j}k}{2z}\rho^2\right)}{\mathrm{j}\lambda z}\iint_{-\infty}^{\infty} U^{\mathrm{src}}(\boldsymbol{\rho}', 0) \times \exp\left(\frac{\mathrm{j}k}{2z}\rho'^2\right)\exp\left(-\frac{\mathrm{j}k}{z}\boldsymbol{\rho}'\cdot\boldsymbol{\rho}\right)\mathrm{d}^2\rho', \tag{1}$$

where $k = 2\pi/\lambda$, λ is the wavelength, $\boldsymbol{\rho} = \hat{\mathbf{x}}x + \hat{\mathbf{y}}y$ is the observation vector, and $\boldsymbol{\rho}' = \hat{\mathbf{x}}x' + \hat{\mathbf{y}}y'$ is the source vector.[11] Applying the transform

$$\iint_{-\infty}^{\infty}\{\cdot\}\exp\left(\frac{\mathrm{j}k}{z}\boldsymbol{\rho}''\cdot\boldsymbol{\rho}\right)\mathrm{d}^2\rho \tag{2}$$

*Address all correspondence to: Milo W. Hyde IV, E-mail: milo.hyde@afit.edu

to both sides of Eq. (1) and simplifying yields

$$\mathrm{j}\lambda z \exp(-\mathrm{j}kz)\iint_{-\infty}^{\infty} U^{\mathrm{obs}}(\boldsymbol{\rho}, z)\exp\left(-\frac{\mathrm{j}k}{2z}\rho^2\right)\exp\left(\frac{\mathrm{j}k}{z}\boldsymbol{\rho}''\cdot\boldsymbol{\rho}\right)\mathrm{d}^2\rho$$
$$= \iint_{-\infty}^{\infty} U^{\mathrm{src}}(\boldsymbol{\rho}', 0)\exp\left(\frac{\mathrm{j}k}{2z}\rho'^2\right)$$
$$\times \iint_{-\infty}^{\infty} \exp\left[-\frac{\mathrm{j}k}{z}(\boldsymbol{\rho}' - \boldsymbol{\rho}'')\cdot\boldsymbol{\rho}\right]\mathrm{d}^2\rho\mathrm{d}^2\rho'. \tag{3}$$

The integral over $\boldsymbol{\rho}$ in Eq. (3) is equal to $\lambda^2 z^2 \delta(\boldsymbol{\rho}' - \boldsymbol{\rho}'')$. Thus, the second line of Eq. (3) evaluates to

$$\lambda^2 z^2 U^{\mathrm{src}}(\boldsymbol{\rho}'', 0)\exp\left(\frac{\mathrm{j}k}{2z}\rho''^2\right). \tag{4}$$

Solving the resulting expression for the source plane field produces

$$U^{\mathrm{src}}(\boldsymbol{\rho}'', 0) = \frac{\exp(-\mathrm{j}kz)\exp\left(-\frac{\mathrm{j}k}{2z}\rho''^2\right)}{-\mathrm{j}\lambda z}$$
$$\times \iint_{-\infty}^{\infty} U^{\mathrm{obs}}(\boldsymbol{\rho}, z)\exp\left(-\frac{\mathrm{j}k}{2z}\rho^2\right)\exp\left(\frac{\mathrm{j}k}{z}\boldsymbol{\rho}''\cdot\boldsymbol{\rho}\right)\mathrm{d}^2\rho. \tag{5}$$

This equation is the inverse Fresnel transform of Eq. (1) and yields the field in the source plane given the field in the observation plane.

The goal here is to find the source plane field that produces the exact observation plane field over a defined RoI. Therefore, let the windowed observation plane field be

$$U^{\mathrm{obs,w}}(\boldsymbol{\rho}, z) = W(\boldsymbol{\rho})U^{\mathrm{obs}}(\boldsymbol{\rho}, z), \tag{6}$$

where W is a window function, e.g., rectangle, circle, etc, which represents the RoI. Substituting Eq. (6) into Eq. (5) produces

$$U^{\mathrm{src,f}}(\boldsymbol{\rho}'', 0) = \frac{\exp(-\mathrm{j}kz)\exp\left(-\frac{\mathrm{j}k}{2z}\rho''^2\right)}{-\mathrm{j}\lambda z}\iint_{-\infty}^{\infty} W(\boldsymbol{\rho})U^{\mathrm{obs}}(\boldsymbol{\rho}, z)$$
$$\times \exp\left(-\frac{\mathrm{j}k}{2z}\rho^2\right)\exp\left(\frac{\mathrm{j}k}{z}\boldsymbol{\rho}''\cdot\boldsymbol{\rho}\right)\mathrm{d}^2\rho, \tag{7}$$

where $U^{\mathrm{src,f}}$ is the desired, spatially filtered source. Substituting Eq. (1) into Eq. (7) and simplifying yields

$$U^{\mathrm{src,f}}(\boldsymbol{\rho}'', 0) = \frac{\exp\left(-\frac{\mathrm{j}k}{2z}\rho''^2\right)}{\lambda^2 z^2}\iint_{-\infty}^{\infty} U^{\mathrm{src}}(\boldsymbol{\rho}', 0)\exp\left(\frac{\mathrm{j}k}{2z}\rho'^2\right)$$
$$\times \iint_{-\infty}^{\infty} W(\boldsymbol{\rho})\exp\left[-\frac{\mathrm{j}k}{z}(\boldsymbol{\rho}' - \boldsymbol{\rho}'')\cdot\boldsymbol{\rho}\right]\mathrm{d}^2\rho\mathrm{d}^2\rho'. \tag{8}$$

The integral on the last line of Eq. (8) is the Fourier transform of the window function W represented hereafter as $\tilde{W}$.

The final result is

$$U^{\mathrm{src,f}}(\boldsymbol{\rho}'', 0) = \frac{\exp\left(-\frac{\mathrm{j}k}{2z}\rho''^2\right)}{\lambda^2 z^2}\iint_{-\infty}^{\infty} U^{\mathrm{src}}(\boldsymbol{\rho}', 0)$$
$$\times \exp\left(\frac{\mathrm{j}k}{2z}\rho'^2\right)\tilde{W}(\boldsymbol{\rho}' - \boldsymbol{\rho}'')\mathrm{d}^2\rho'. \tag{9}$$

The Fresnel filtered source is the true source multiplied by a quadratic phase factor correlated with $\tilde{W}$. Evaluating Eq. (9) yields the source plane field that produces the exact observation plane field over the RoI W. Note that the filtered observation plane field will be nonphysical outside the RoI.

2.2 *Fresnel Filtering Discussion*

If the observation plane is in the far-zone, Eq. (9) simplifies to

$$U^{\mathrm{src,f}}(\boldsymbol{\rho}'', 0) = \frac{\exp\left(-\frac{\mathrm{j}k}{2z}\rho''^2\right)}{\lambda^2 z^2}$$
$$\times \iint_{-\infty}^{\infty} U^{\mathrm{src}}(\boldsymbol{\rho}', 0)\tilde{W}(\boldsymbol{\rho}' - \boldsymbol{\rho}'')\mathrm{d}^2\rho', \tag{10}$$

which can be considered the Fraunhofer filtered source. If W is rectangular, as it often is, then Eq. (9) becomes

$$U^{\mathrm{src,f}}(\boldsymbol{\rho}'', 0) = \frac{\exp\left(-\frac{\mathrm{j}k}{2z}\rho''^2\right)}{\lambda^2 z^2}\iint_{-\infty}^{\infty} U^{\mathrm{src}}(\boldsymbol{\rho}', 0)\exp\left(\frac{\mathrm{j}k}{2z}\rho'^2\right)$$
$$\times W_x W_y \mathrm{sinc}\left[\frac{k}{z}\frac{W_x}{2}(x' - x'')\right]\mathrm{sinc}\left[\frac{k}{z}\frac{W_y}{2}(y' - y'')\right]\mathrm{d}x'\mathrm{d}y', \tag{11}$$

where W_y and W_x are the height and width of the RoI and $\mathrm{sinc}(x) = \sin(x)/x$.

A spatially broadband source often encountered in practice is a point source. Letting $U^{\mathrm{src}}(\boldsymbol{\rho}', 0) = \delta(\boldsymbol{\rho}' - \boldsymbol{\rho}_c)$ and evaluating the integrals in Eq. (11) yields

$$U^{\mathrm{src,f}}(\boldsymbol{\rho}, 0) = \frac{W_x W_y}{\lambda^2 z^2}\exp\left[-\frac{\mathrm{j}k}{2z}(\rho^2 - \rho_c^2)\right]$$
$$\times \mathrm{sinc}\left[\frac{k}{z}\frac{W_x}{2}(x_c - x)\right]\mathrm{sinc}\left[\frac{k}{z}\frac{W_y}{2}(y_c - y)\right], \tag{12}$$

where $\boldsymbol{\rho}_c = \hat{\mathbf{x}}x_c + \hat{\mathbf{y}}y_c$ is the location of the point source in the source plane. Equation (12) is the sinc point source model discussed in Ref. 1.

In most cases, Eq. (9) cannot be evaluated in closed form. Thus, the integral must be computed numerically or approximated. The former is generally undesired because the sampling requirements to represent U^{src} on a discrete grid are prohibitive, hence wanting to filter U^{src}.

The latter, approximating Eq. (9), is a very good option for highly divergent fields, like fields transiting negative lenses or reflected from convex mirrors. In these scenarios, Eq. (9) can be evaluated using the method of stationary phase (MoSP).[12] Let $U^{\mathrm{src}}(\boldsymbol{\rho}', 0) = A(\boldsymbol{\rho}')\exp[\mathrm{j}k/(2R)\rho'^2]$, where A is the amplitude of U^{src} and $R > 0$ is the curvature.

Substituting this into Eq. (9) and evaluating the integrals using the MoSP produces

$$U^{\mathrm{src,f}}(\boldsymbol{\rho},0) \approx \frac{\exp\left(-\frac{\mathrm{j}k}{2z}\rho^2\right)}{-\mathrm{j}\lambda z}\frac{A(0)\tilde{W}(-\boldsymbol{\rho})}{1+z/R}. \tag{13}$$

The accuracy of Eq. (13) improves as $R \to 0$ and is generally good for $R < z/10$.

Unfortunately, Eq. (9) cannot be easily evaluated or approximated when simulating spatially broadband fields with random wavefronts, like fields reflected from rough surfaces. By far, the most popular approach for simulating fields scattered from rough surfaces is to model the scattered field as $U^{\mathrm{src}}(\boldsymbol{\rho}',0) = A(\boldsymbol{\rho}')\exp[\mathrm{j}k\phi(\boldsymbol{\rho}')]$, where ϕ is a delta-correlated random phase screen with values uniformly distributed between $-\pi$ and π. Equation (9) is then evaluated numerically to yield $U^{\mathrm{src,f}}$.[3] This model for the field scattered from a rough surface is accurate if the surface height standard deviation $\sigma_h > \lambda$ and the surface's correlation radius $l_h < \Delta$, where Δ is the grid spacing. Although these conditions are often met in practice, the statistics of the rough surface, i.e., σ_h and l_h, are not included in the model. Note that when using the delta-correlated, $-\pi$-to-π phase screen model for simulating rough surface scattering, $l_h = \Delta$, where Δ is the grid spacing.

Another lesser known approach, which includes σ_h and l_h, is to assume that $A(\boldsymbol{\rho}') \approx A_x(x')A_y(y')$, likewise for $\tilde{W}$, and $h(\boldsymbol{\rho}') \approx h_x(x') + h_y(y')$. Equation (9) then simplifies to

$$\begin{aligned} U^{\mathrm{src,f}}(\boldsymbol{\rho},0) &\approx U_x^{\mathrm{src,f}}(x,0)U_y^{\mathrm{src,f}}(y,0) \\ U_\alpha^{\mathrm{src,f}}(\alpha,0) &= \frac{\exp\left(-\frac{\mathrm{j}k}{2z}\alpha^2\right)}{\lambda z} \\ &\times \int_{-\infty}^{\infty} A_\alpha(\alpha')\exp\left\{\mathrm{j}k\left[\frac{\alpha'^2}{2z}+h_\alpha(\alpha')\right]\right\}\tilde{W}_\alpha(\alpha'-\alpha)\mathrm{d}\alpha', \end{aligned} \tag{14}$$

where $\alpha = x, y$. Because of the reduction in dimensionality, it is now practical to synthesize two independent one-dimensional (1-D) instances of h and to evaluate Eq. (14) numerically. The resulting independent 1-D $U_x^{\mathrm{src,f}}$ and $U_y^{\mathrm{src,f}}$ can be downsampled, expanded to two-dimensional (2-D) grids, and then multiplied together to form $U^{\mathrm{src,f}}$. This approach can also be used to filter fields with highly curved random wavefronts, e.g., fields reflected from rough convex surfaces. By letting $h(\boldsymbol{\rho}') = h_x(x') + h_y(y')$, the simulated l_h is not equal to the desired l_h and, in general, the statistics of the simulated rough surface are inhomogeneous and anisotropic.

As a consequence of Eq. (9), both rough surface filtering approaches mentioned above filter the random source field directly, so the filtered source, after propagation, is equal to U^{obs} over the RoI. For simulations involving random fields, the fact that this particular filtered source produces the exact same U^{obs} (over the RoI) as this particular unfiltered, spatially broadband source is generally inconsequential. What is important is that the filtered U^{obs} be representative of the true, unfiltered U^{obs}, i.e., the statistics of the filtered and unfiltered U^{obs} match. This new statistical filtering approach is presented in the next section.

2.3 *Filtering Quasihomogeneous Sources*

Quasihomogeneous sources are a subclass of the more general and popular Schell-model sources.[12,13] The intensity I of a quasihomogeneous source varies slowly compared to its complex degree of spatial coherence μ, such that its mutual intensity J takes the approximate form[12,13]

$$\begin{aligned} J(\boldsymbol{\rho}_1,\boldsymbol{\rho}_2) &= \langle U(\boldsymbol{\rho}_1)U^*(\boldsymbol{\rho}_2)\rangle = A(\boldsymbol{\rho}_1)A(\boldsymbol{\rho}_2)\mu(\boldsymbol{\rho}_1-\boldsymbol{\rho}_2) \\ &\approx I\left(\frac{\boldsymbol{\rho}_1+\boldsymbol{\rho}_2}{2}\right)\mu(\boldsymbol{\rho}_1-\boldsymbol{\rho}_2), \end{aligned} \tag{15}$$

where $I = |A|^2$. Equation (15) is a good statistical model for light scattered from rough targets, where the spot on the target' rough surface is much wider than the surface's autocorrelation function.

The goal here is to find the filtered mutual intensity $J^{\mathrm{src,f}}$, which when propagated will produce the exact mutual intensity J^{obs} over the RoI. From $J^{\mathrm{src,f}}$, one can then synthesize instances of $U^{\mathrm{src,f}}$ for use in optical simulations.

Taking the autocorrelation of Eq. (9) yields

$$\begin{aligned} J^{\mathrm{src,f}}(\boldsymbol{\rho}_1,\boldsymbol{\rho}_2) &= \frac{\exp\left[-\frac{\mathrm{j}k}{2z}(\rho_1^2-\rho_2^2)\right]}{\lambda^4 z^4} \\ &\times \iiiint_{-\infty}^{\infty} J^{\mathrm{src}}(\boldsymbol{\rho}_1',\boldsymbol{\rho}_2')\exp\left[\frac{\mathrm{j}k}{2z}(\rho_1'^2-\rho_2'^2)\right] \\ &\times \tilde{W}(\boldsymbol{\rho}_1'-\boldsymbol{\rho}_1)\tilde{W}^*(\boldsymbol{\rho}_2'-\boldsymbol{\rho}_2)\mathrm{d}^2\rho_1'\mathrm{d}^2\rho_2'. \end{aligned} \tag{16}$$

Assuming that U^{src} is a quasihomogeneous random field, i.e., the form of J^{src} is given by Eq. (15), and using the integral expression for $\tilde{W}$ given in Eq. (8) transforms Eq. (16) into

$$\begin{aligned} J^{\mathrm{src,f}}(\boldsymbol{\rho}_1,\boldsymbol{\rho}_2) &= \frac{\exp\left[-\frac{\mathrm{j}k}{2z}(\rho_1^2-\rho_2^2)\right]}{\lambda^4 z^4} \\ &\times \iiiint_{-\infty}^{\infty} W(\boldsymbol{\rho}_1'')W^*(\boldsymbol{\rho}_2'')\exp\left[\frac{\mathrm{j}k}{z}(\boldsymbol{\rho}_1\cdot\boldsymbol{\rho}_1''-\boldsymbol{\rho}_2\cdot\boldsymbol{\rho}_2'')\right] \\ &\times \iiiint_{-\infty}^{\infty} I\left(\frac{\boldsymbol{\rho}_1'+\boldsymbol{\rho}_2'}{2}\right)\mu(\boldsymbol{\rho}_1'-\boldsymbol{\rho}_2')\exp\left[\frac{\mathrm{j}k}{2z}(\rho_1'^2-\rho_2'^2)\right] \\ &\times \exp\left[-\frac{\mathrm{j}k}{z}(\boldsymbol{\rho}_1''\cdot\boldsymbol{\rho}_1'-\boldsymbol{\rho}_2''\cdot\boldsymbol{\rho}_2')\right]\mathrm{d}^2\rho_1'\mathrm{d}^2\rho_2'\mathrm{d}^2\rho_1''\mathrm{d}^2\rho_2''. \end{aligned} \tag{17}$$

To make further progress, it is necessary to assume that the observation plane is in the far-zone of the quasihomogeneous source. This initially seems like a very prohibitive condition; however, the far-zone criterion for quasihomogeneous sources is typically far less restrictive than that for coherent sources. The far-zone criterion for quasihomogeneous sources is given by Goodman[13] and Gori[14]

$$z > \frac{2Dd_c}{\lambda}, \tag{18}$$

where D, in this context, is the diameter of the illuminated area on the target and d_c is the spatial coherence diameter of the field scattered from the target. Since typically $d_c < 10\lambda$,

one obtains the far-zone J only a short distance away from the target's surface.

Assuming that Eq. (18) is satisfied and making the common variable substitutions $\mathbf{s} = \boldsymbol{\rho}_1' - \boldsymbol{\rho}_2'$ and $\mathbf{t} = (\boldsymbol{\rho}_1' + \boldsymbol{\rho}_2')/2$ simplifies Eq. (17) to

$$J^{\mathrm{src,f}}(\boldsymbol{\rho}_1, \boldsymbol{\rho}_2) \approx \frac{\exp\left[-\frac{\mathrm{j}k}{2z}(\rho_1^2 - \rho_2^2)\right]}{\lambda^4 z^4} \times \iiiint_{-\infty}^{\infty} W(\boldsymbol{\rho}_1'')W^*(\boldsymbol{\rho}_2'') \exp\left[\frac{\mathrm{j}k}{z}(\boldsymbol{\rho}_1 \cdot \boldsymbol{\rho}_1'' - \boldsymbol{\rho}_2 \cdot \boldsymbol{\rho}_2'')\right] \times \iint_{-\infty}^{\infty} I(\mathbf{t}) \exp\left[-\frac{\mathrm{j}k}{z}(\boldsymbol{\rho}_1'' - \boldsymbol{\rho}_2'') \cdot \mathbf{t}\right] \mathrm{d}^2 t \times \iint_{-\infty}^{\infty} \mu(\mathbf{s}) \exp\left[-\frac{\mathrm{j}k}{z}\left(\frac{\boldsymbol{\rho}_1'' + \boldsymbol{\rho}_2''}{2}\right) \cdot \mathbf{s}\right] \mathrm{d}^2 s \mathrm{d}^2 \rho_1'' \mathrm{d}^2 \rho_2''. \tag{19}$$

Note that the product of the $\mathbf{t}$ and $\mathbf{s}$ integrals is the generalized Van Cittert–Zernike theorem applied to J^{src}.[12,13] Substituting $\tilde{I}$ and $\tilde{\mu}$ for the Fourier transforms of I and μ, respectively, yields

$$J^{\mathrm{src,f}}(\boldsymbol{\rho}_1, \boldsymbol{\rho}_2) = \frac{\exp\left[-\frac{\mathrm{j}k}{2z}(\rho_1^2 - \rho_2^2)\right]}{\lambda^4 z^4} \times \iiiint_{-\infty}^{\infty} W(\boldsymbol{\rho}_1'')W^*(\boldsymbol{\rho}_2'')\tilde{\mu}\left(\frac{\boldsymbol{\rho}_1'' + \boldsymbol{\rho}_2''}{2}\right) \times \tilde{I}(\boldsymbol{\rho}_1'' - \boldsymbol{\rho}_2'') \exp\left[\frac{\mathrm{j}k}{z}(\boldsymbol{\rho}_1 \cdot \boldsymbol{\rho}_1'' - \boldsymbol{\rho}_2 \cdot \boldsymbol{\rho}_2'')\right] \mathrm{d}^2 \rho_1'' \mathrm{d}^2 \rho_2''. \tag{20}$$

The integrand in Eq. (20) is a new J (physically, a new partially coherent source) with the product of W, W^*, and $\tilde{\mu}$ serving as the source's shape and $\tilde{I}$ as the source's coherence function. If U^{src} is a circular complex Gaussian, as it is for rough surface scattering (fully developed speckle), then the width of $\tilde{I}$ is the mean speckle size.[15] In most simulations involving speckle, the RoI contains many speckles. Note that the RoI, in general, is not the same as the pupil or detector areas. Thus, $\tilde{I}$ is much narrower than the product of W, W^*, and $\tilde{\mu}$, and the integrand in Eq. (20) is another quasihomogeneous source.

Making the variable substitutions $\mathbf{s} = \boldsymbol{\rho}_1'' - \boldsymbol{\rho}_2''$ and $\mathbf{t} = (\boldsymbol{\rho}_1'' + \boldsymbol{\rho}_2'')/2$ and evaluating the integrals produces

$$J^{\mathrm{src,f}}(\boldsymbol{\rho}_1, \boldsymbol{\rho}_2) \approx \frac{\exp\left[-\frac{\mathrm{j}k}{2z}(\rho_1^2 - \rho_2^2)\right]}{\lambda^4 z^4} \tilde{\tilde{I}}\left(\frac{\boldsymbol{\rho}_1 + \boldsymbol{\rho}_2}{2}\right) \tilde{\mathcal{W}}(\boldsymbol{\rho}_1 - \boldsymbol{\rho}_2), \tag{21}$$

where $\tilde{\tilde{I}} = \lambda^2 z^2 I$ and

$$\tilde{\mathcal{W}}(\boldsymbol{\rho}_1 - \boldsymbol{\rho}_2) \approx \iint_{-\infty}^{\infty} |W(\mathbf{t})|^2 \tilde{\mu}(\mathbf{t}) \exp\left[\frac{\mathrm{j}k}{z}(\boldsymbol{\rho}_1 - \boldsymbol{\rho}_2) \cdot \mathbf{t}\right] \mathrm{d}^2 t. \tag{22}$$

The final simplified result is

$$J^{\mathrm{src,f}}(\boldsymbol{\rho}_1, \boldsymbol{\rho}_2) = \frac{\exp\left[-\frac{\mathrm{j}k}{2z}(\rho_1^2 - \rho_2^2)\right]}{\lambda^2 z^2} \times I\left(\frac{\boldsymbol{\rho}_1 + \boldsymbol{\rho}_2}{2}\right) \tilde{\mathcal{W}}(\boldsymbol{\rho}_1 - \boldsymbol{\rho}_2). \tag{23}$$

From Eq. (23), an instance of $U^{\mathrm{src,f}}$ is given by

$$U^{\mathrm{src,f}}(\boldsymbol{\rho}) = \frac{\exp\left(-\frac{\mathrm{j}k}{2z}\rho^2\right)}{\lambda z} A(\boldsymbol{\rho}) T(\boldsymbol{\rho}), \tag{24}$$

where T is a complex amplitude screen whose autocorrelation function is $\tilde{W}$. The most straightforward and numerically efficient method for synthesizing T is the Monte Carlo spectral method (MCSM).[16–20] The method uses the power spectral density (PSD) to filter or color an array of delta-correlated complex Gaussian random numbers in the frequency domain.

The applicable PSD can be derived from $\tilde{W}$ by applying the Wiener–Khinchin theorem.[12,13] Fourier transforming Eq. (22) and simplifying produces

$$\mathcal{S}(\mathbf{f}) = \iint_{-\infty}^{\infty} \tilde{\mathcal{W}}(\boldsymbol{\Delta\rho}) \exp(-\mathrm{j}2\pi \mathbf{f} \cdot \boldsymbol{\Delta\rho}) \mathrm{d}^2 \Delta\rho = \lambda^2 z^2 |W(\lambda z \mathbf{f})|^2 \tilde{\mu}(\lambda z \mathbf{f}), \tag{25}$$

where $\boldsymbol{\Delta\rho} = \boldsymbol{\rho}_1 - \boldsymbol{\rho}_2$ and $\mathbf{f} = \hat{\mathbf{x}} f_x + \hat{\mathbf{y}} f_y$ is the spatial frequency vector. In general, $\mathcal{S}$ given in Eq. (25) is not normalized, i.e., the volume under $\mathcal{S}$ is not one.[13] This is only a minor mathematical inconvenience; it has no effect on synthesizing T.

Notice that in contrast to Fresnel spatial filtering [see Eq. (9)], quasihomogeneous spatial filtering does not use U^{src} directly. Most importantly, the spatially broadband U^{src} is never discretized, meaning that quasihomogeneous filtering typically requires far fewer grid points than Eq. (9).

3 Validation

3.1 *Simulation Details and Methodology*

It is best to present the utility of the above analysis through example. Here, the transmission and subsequent propagation of a collimated Gaussian beam through a ground glass diffuser was simulated. The simulation was performed in 1-D, so the results using Eq. (24) could be directly compared to those using the unfiltered, spatially broadband U^{src} and Eq. (9)—the sampling requirements to propagate U^{src} were impractical using 2-D grids.

The source field for this simulation was

$$U^{\mathrm{src}}(x) = \exp\left(-\frac{x^2}{\sigma^2}\right) \mathrm{rect}\left(\frac{x}{D}\right) \exp[\mathrm{j}kh(x)], \tag{26}$$

where $\lambda = 1\ \mu$m, $\sigma = 5$ mm, $D = 25.4$ mm, rect is the rectangle function defined by Goodman,[11] and h is the diffuser's optical path length function. The path lengths h were assumed to be Gaussian distributed and Gaussian correlated with a standard deviation $\sigma_h = 3\ \mu$m and a correlation length $l_h = 60\ \mu$m. Instances of h were produced using the MCSM.

Equation (26) and the two filtered sources discussed below were propagated $z = 15$ m (corresponding to a 1-D Fresnel number $N_F \approx 3.3$) in eight steps to the observation plane using the angular spectrum method.[1,2] The source and observation planes were discretized using 239,884 points with 3 and 11 μm sample spacings, respectively. The RoI in the observation plane was $W_x = 10$ cm wide.

The Fresnel-filtered source was computed directly from Eq. (26) using a 1-D form of Eq. (9), namely,

$$U^{\mathrm{src,f}}(x) = \frac{\exp\left(-\frac{\mathrm{j}k}{2z}x^2\right)}{\lambda z} \times \int_{-\infty}^{\infty} \exp\left(-\frac{x'^2}{\sigma^2}\right)\mathrm{rect}\left(\frac{x'}{D}\right)\exp[\mathrm{j}kh(x')] \times \exp\left(\frac{\mathrm{j}k}{2z}x'^2\right) W_x \mathrm{sinc}\left[\frac{k}{z}\frac{W_x}{2}(x'-x)\right]\mathrm{d}x'. \quad (27)$$

An instance of the quasihomogeneous filtered source was

$$U^{\mathrm{src,f}}(x) = \frac{\exp\left(-\frac{\mathrm{j}k}{2z}x^2\right)}{\sqrt{\lambda z}}\exp\left(-\frac{x^2}{\sigma^2}\right)\mathrm{rect}\left(\frac{x}{D}\right)T(x), \quad (28)$$

where T was synthesized from the following 1-D PSD

$$\mathcal{S}(f) = \lambda z \mathrm{rect}\left(\frac{\lambda z f}{W_x}\right)\sqrt{\pi}\frac{l_h}{k\sigma_h}\exp\left[-\left(\frac{l_h \lambda f}{2\sigma_h}\right)^2\right] \quad (29)$$

using the MCSM. The PSD of T requires computing the moment $\langle \exp[\mathrm{j}kh(x_1)]\exp[-\mathrm{j}kh(x_2)]\rangle$. For Gaussian distributed and Gaussian correlated h, this moment is approximately

$$\langle \exp[\mathrm{j}kh(x_1)]\exp[-\mathrm{j}kh(x_2)]\rangle \approx \exp\left[-k^2\sigma_h^2\frac{(x_1-x_2)^2}{l_h^2}\right] \quad (30)$$

assuming that $\sigma_h > \lambda$, which is generally the case. Note that $l_h/(k\sigma_h)$ is the approximate spatial coherence radius of the scattered field.

It is important to note that the large number of points and small spacings mentioned above were required to perform the propagation simulations with the source plane fields given in Eqs. (26) and (27). Synthesizing and propagating Eq. (28) requires significantly less resources and, if desired, can easily be done in 2-D. For example, the same simulation described above using Eq. (28) requires only 2048 points and 80 μm spacings in both the source and observation planes. In addition, the 15-m propagation can be performed in three steps instead of eight.

3.2 *Simulation Results*

Figures 1–3 show the results. Figure 1 shows instances of U^{src} [Eq. (26), Figs. 1(a) and 1(b)], $U^{\mathrm{src,f}}$ [Eq. (27),

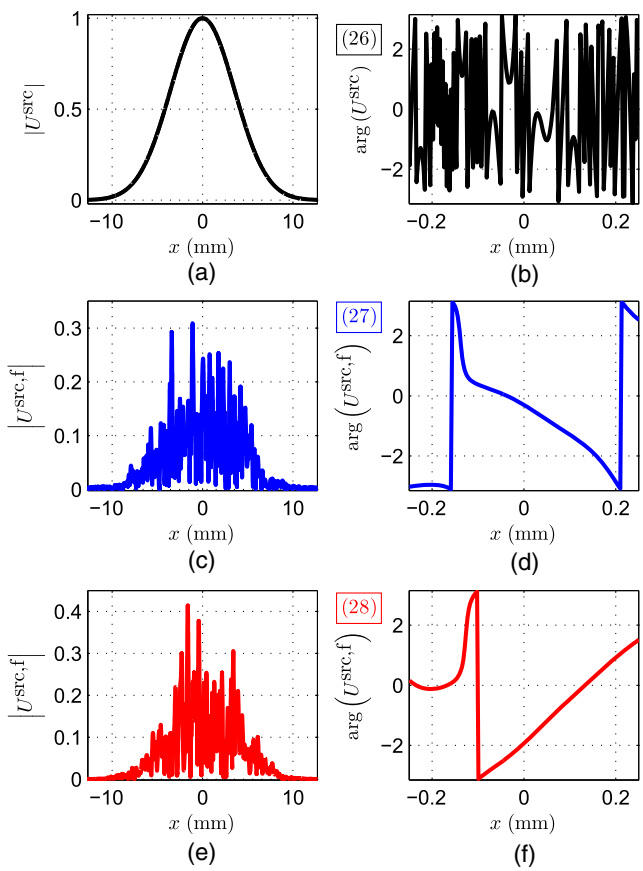

Fig. 1 Magnitude and phase of source plane field instances U^{src} given by (a, b) Eq. (26), (c, d) Eq. (27), and (e, f) Eq. (28).

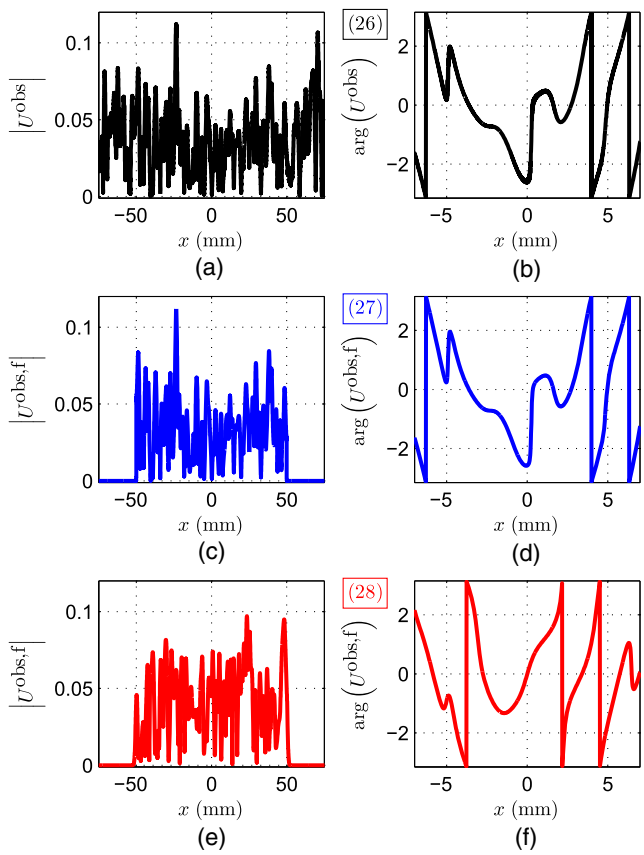

Fig. 2 Magnitude and phase of observation plane fields U^{obs} corresponding to the instances given by (a, b) Eq. (26), (c, d) Eq. (27), and (e, f) Eq. (28).

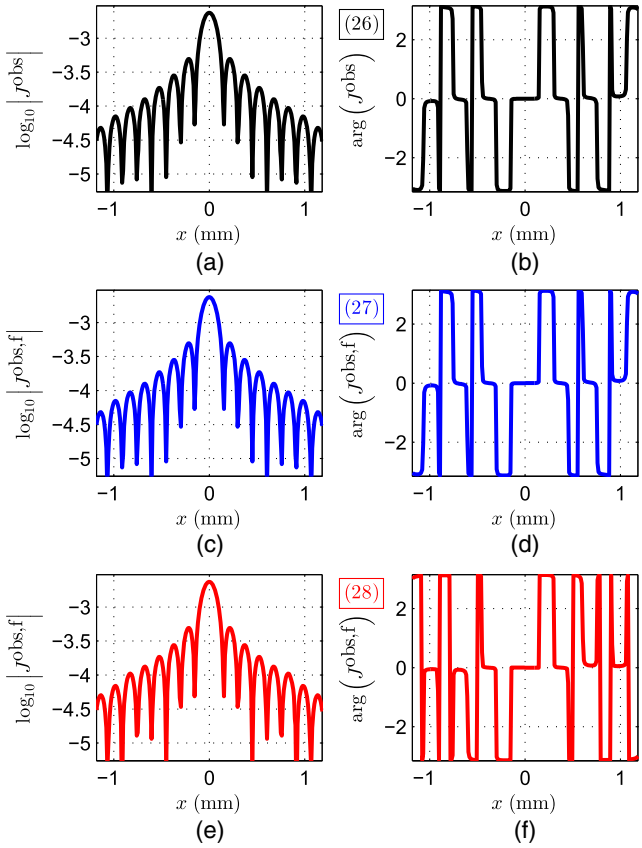

Fig. 3 Log magnitude and phase of observation plane mutual intensities J^{obs} computed from 2500 propagated instances of (a, b) U^{src} Eq. (26), (c, d) Eq. (27), and (e, f) Eq. (28).

Figs. 1(c) and 1(d)], and $U^{\mathrm{src,f}}$ [Eq. (28), Figs. 1(e) and 1(f)]. The effects of filtering are quite clear in Figs. 1(d) and 1(f), where the filtered phases (or wavefronts) are much smoother than the [Eq. (26)] result [Fig. 1(b)].

Figure 2 shows the corresponding U^{obs} instances. As expected, the U^{obs} corresponding to Eq. (26) [(a) and (b)] and Eq. (27) [(c) and (d)] are identical over the RoI; Eq. (27) is nonphysical outside the RoI. The U^{obs} corresponding to Eq. (28) [(e) and (f)] is different than the other two. Recall that the goal here is to ensure that the U^{obs} obtained from propagating Eq. (28) is representative of Eqs. (26) and (27), not necessary equal.

To show this, Fig. 3 reports the observation plane mutual intensities J^{obs} computed over the RoI from 2500 instances of U^{obs} corresponding to source fields Eq. (26) [(a) and (b)], Eq. (27) [(c) and (d)], and Eq. (28) [(e) and (f)]. Except for very minor disagreements in the locations of phase wrapping cuts [Fig. 3(f)], caused by small numerical differences in the positions of J^{obs} zero crossings [notice that the wrapping cut discrepancies occur at the "nulls" in the $\log_{10}|J^{\mathrm{obs}}|$ plot [Fig. 3(e)], the curves are in excellent agreement. Figure 3 validates the quasihomogeneous filtering approach discussed in Sec. 2.

4 Conclusion

In this a paper, two-source plane spatial filtering techniques for use in wave optics simulations were presented and discussed. The first, called Fresnel spatial filtering, provided the spatially band-limited source $U^{\mathrm{src,f}}$ that produced the exact same U^{obs} over a specified RoI as the original, spatially broadband U^{src}. In general, the Fresnel spatial filtering integral could not be evaluated analytically. Evaluating the integral numerically was undesirable because the number of points and sample spacing required to accurately represent U^{src} were onerous.

This motivated development of the second filtering technique—statistical or quasihomogeneous spatial filtering. Instead of requiring that $U^{\mathrm{src,f}}$ produces the exact same U^{obs} over the RoI as U^{src}, this approach only required that the filtered source produces a U^{obs} that was representative of that produced by U^{src} (i.e., the statistics of the filtered and unfiltered U^{obs} matched), making this approach very applicable in simulations involving scattering from rough surfaces or transmission through diffusers. Because U^{src} never needed to be discretized, this statistical approach required far fewer points than Fresnel spatial filtering. In addition, the quasihomogeneous spatial filtering approach included the underlying statistical properties of the random scatterer, i.e., σ_h and l_h. This stood in contrast to the more common method of using a delta-correlated, $-\pi$-to-π phase screen for modeling rough surface scattering or transmission through diffusers.

Both Fresnel and quasihomogeneous spatial filtering were validated in Sec. 3. For this purpose, the near-zone propagation of light transmitted by a ground glass diffuser was simulated. The results obtained using both filtering approaches were compared to those of the original U^{src}. All were in excellent agreement.

The spatial filtering techniques discussed in this paper will be useful for mitigating aliasing in wave optics simulations involving spatially broadband fields, e.g., simulating rough surface scattering, speckle, etc. These scenarios or optical phenomena are often encountered in the deployment of optical phased arrays, high-energy lasers, active imaging and remote sensing systems, and medicine. Thus, the spatial filtering techniques presented herein will be applicable in the design and subsequent simulation of those systems. In addition, these techniques can also be used in laboratory experiments where spatial light modulators serve as filtered rough targets. This approach has many advantages over using actual rough, diffuse objects—the main one being light conservation.

Acknowledgments

The views expressed in this paper are those of the authors and do not reflect the official policy or position of the US Air Force, the Department of Defense, or the US government.

References

1. J. D. Schmidt, *Numerical Simulation of Optical Wave Propagation with Examples in MATLAB*, SPIE Press, Bellingham, Washington (2010).
2. D. G. Voelz, *Computational Fourier Optics: A MATLAB Tutorial*, SPIE Press, Bellingham, Washington (2011).
3. S. C. Coy and B. P. Venet, *WaveTrain User Guide*, MZA Associates Corporation, Albuquerque, New Mexico (2011).
4. D. G. Voelz and M. C. Roggemann, "Digital simulation of scalar optical diffraction: revisiting chirp function sampling criteria and consequences," *Appl. Opt.* **48**, 6132–6142 (2009).
5. F. Shen and A. Wang, "Fast-Fourier-transform based numerical integration method for the Rayleigh-Sommerfeld diffraction formula," *Appl. Opt.* **45**, 1102–1110 (2006).
6. D. P. Kelly, "Numerical calculation of the Fresnel transform," *J. Opt. Soc. Am. A* **31**, 755–764 (2014).

7. K. Matsushima and T. Shimobaba, "Band-limited angular spectrum method for numerical simulation of free-space propagation in far and near fields," *Opt. Express* **17**, 19662–19673 (2009).
8. K. Matsushima, "Shifted angular spectrum method for off-axis numerical propagation," *Opt. Express* **18**, 18453–18463 (2010).
9. X. Yu et al., "Band-limited angular spectrum numerical propagation method with selective scaling of observation window size and sample number," *J. Opt. Soc. Am. A* **29**, 2415–2420 (2012).
10. K. Falaggis, T. Kozacki, and M. Kujawinska, "Computation of highly off-axis diffracted fields using the band-limited angular spectrum method with suppressed Gibbs related artifacts," *Appl. Opt.* **52**, 3288–3297 (2013).
11. J. W. Goodman, *Introduction to Fourier Optics*, 3rd ed., Roberts & Company, Englewood, Colorado (2005).
12. L. Mandel and E. Wolf, *Optical Coherence and Quantum Optics*, Cambridge University, New York (1995).
13. J. W. Goodman, *Statistical Optics*, 2nd ed., Wiley, Hoboken, New Jersey (2015).
14. F. Gori, "Far-zone approximation for partially coherent sources," *Opt. Lett.* **30**, 2840–2842 (2005).
15. J. W. Goodman, *Speckle Phenomena in Optics: Theory and Applications*, Roberts & Company, Englewood, Colorado (2007).
16. D. Voelz, X. Xiao, and O. Korotkova, "Numerical modeling of Schell-model beams with arbitrary far-field patterns," *Opt. Lett.* **40**, 352–355 (2015).
17. M. W. Hyde et al., "Experimentally generating any desired partially coherent Schell-model source using phase-only control," *J. Appl. Phys.* **118**(9), 093102 (2015).
18. C. A. Mack, "Generating random rough edges, surfaces, and volumes," *Appl. Opt.* **52**, 1472–1480 (2013).
19. H. T. Yura and S. G. Hanson, "Digital simulation of an arbitrary stationary stochastic process by spectral representation," *J. Opt. Soc. Am. A* **28**, 675–685 (2011).
20. H. T. Yura and S. G. Hanson, "Digital simulation of two-dimensional random fields with arbitrary power spectra and non-Gaussian probability distribution functions," *Appl. Opt.* **51**, C77–C83 (2012).

Milo W. Hyde IV received his BS degree in computer engineering from Georgia Tech in 2001 and his MS degree and PhD in electrical engineering from AFIT in 2006 and 2010, respectively. Currently, he is an associate professor in the Department of Electrical and Computer Engineering at AFIT. He is a senior member of IEEE and SPIE. He is also a member of OSA, AGU, DEPS, and ACES.

Santasri R. Bose-Pillai received her PhD in electrical engineering with a focus in optics in 2008 and her MSEE degree in 2005, both from New Mexico State University. She received her BSEE degree with honors from Jadavpur University, India, in 2000. Currently, she is a research assistant professor at AFITs Center for Directed Energy within the Engineering Physics Department. She is a senior member of SPIE. She is also a member of OSA and DEPS.